Form and flow of the Academy of Sciences Ice Cap, Severnaya Zemlya, Russian High Arctic

J. A. Dowdeswell,[1] R. P. Bassford,[2] M. R. Gorman,[1] M. Williams,[3] A. F. Glazovsky,[4] Y. Y. Macheret,[4] A. P. Shepherd,[5] Y. V. Vasilenko,[6] L. M. Savatyuguin,[7] H.-W. Hubberten,[8] and H. Miller[8]

Received 28 December 2000; revised 10 July 2001; accepted 14 July 2001; published 20 April 2002.

[1] The 5,575-km^2 Academy of Sciences Ice Cap is the largest in the Russian Arctic. A 100-MHz airborne radar, digital Landsat imagery, and satellite synthetic aperture radar (SAR) interferometry are used to investigate its form and flow, including the proportion of mass lost through iceberg calving. The ice cap was covered by a 10-km-spaced grid of radar flight paths, and the central portion was covered by a grid at 5-km intervals: a total of 1,657 km of radar data. Digital elevation models (DEMs) of ice surface elevation, ice thickness, and bed elevation data sets were produced (cell size 500 m). The DEMs were used in the selection of a deep ice core drill site. Total ice cap volume is 2,184 km^3 ($\sim$5.5 mm sea level equivalent). The ice cap has a single dome reaching 749 m. Maximum ice thickness is 819 m. About 200 km, or 42%, of the ice margin is marine. About 50% of the ice cap bed is below sea level. The central divide of the ice cap and several major drainage basins, in the south and east of the ice cap and of up to 975 km^2, are delimited from satellite imagery. There is no evidence of past surge activity on the ice cap. SAR interferometric fringes and phase-unwrapped velocities for the whole ice cap indicate slow flow in the interior and much of the margin, punctuated by four fast flowing features with lateral shear zones and maximum velocity of 140 m yr^{-1}. These ice streams extend back into the slower moving ice to within 5–10 km of the ice cap crest. They have lengths of 17–37 km and widths of 4–8 km. Mass flux from these ice streams is $\sim$0.54 km^3 yr^{-1}. Tabular icebergs up to $\sim$1.7 km long are produced. Total iceberg flux from the ice cap is $\sim$0.65 km^3 yr^{-1} and probably represents $\sim$40% of the overall mass loss, with the remainder coming from surface melting. Driving stresses are generally lowest (<40 kPa) close to the ice cap divides and in several of the ice streams. Ice stream motion is likely to include a significant basal component and may involve deformable marine sediments. *INDEX TERMS:* 1827 Hydrology: Glaciology (1863); 6924 Radio Science: Interferometry; 9315 Information Related to Geographic Region: Arctic region; 1863 Hydrology: Snow and ice (1827)

1. Introduction

[2] The ice caps of the Eurasian High Arctic include those on the Russian archipelagos of Severnaya Zemlya, Franz Josef Land, and Novaya Zemlya together with Norwegian Svalbard (Figure 1). The glacier ice on these Arctic islands covers an area of $\sim$92,000 km^2, which is approaching 20% of the ice outside the Antarctic and Greenland ice sheets [*Dowdeswell*, 1995]. There is a steep climatic gradient across the Eurasian High Arctic, from relatively warmer and more moist conditions on Svalbard in the west, where there is a strong northward transfer of heat in ocean currents and storm tracks up the Norwegian and Greenland Seas, to progressively colder and drier conditions farther east. The 18,300 km^2 of ice caps on Severnaya Zemlya represent the easternmost ice masses of any significant size on this environmental gradient across the Eurasian Arctic which is, in turn, predicted by general circulation models to be a region of enhanced future warming [e.g., *Cattle and Crossley*, 1995].

[3] In this paper, the form and flow of the Academy of Sciences Ice Cap, on Komsomolets Island in the Severnaya Zemlya archipelago (Figure 1), are investigated using several airborne and satellite geophysical instruments in order to provide information on (1) ice cap mass balance, particularly quantitative values for mass loss through iceberg production; (2) boundary conditions for ice sheet numerical modeling of ice cap response to climate change; and (3) ice thickness, bed topographic, and ice flow data, important in site selection for a deep ice core. The ice cap, at 5,575 km^2, is the largest in Severnaya Zemlya and, indeed, in the Russian Arctic [*Dowdeswell et al.*, 2001]. We use an airborne ice-penetrating radar, operating at 100 MHz, to measure the surface topography, ice thickness, and bed elevations of this ice cap. These data are then used in combination with digital Landsat imagery to define ice cap drainage basins, and with ice surface velocities

[1]Scott Polar Research Institute, University of Cambridge, Lensfield Road, Cambridge, England, United Kingdom.
[2]Centre for Polar Observation and Modelling, Bristol Glaciology Centre, School of Geographical Sciences, University of Bristol, Bristol, England, United Kingdom.
[3]Department of Geomatics, University of Newcastle, Newcastle-upon-Tyne, England, United Kingdom.
[4]Institute of Geography, Russian Academy of Sciences, Moscow, Russia.
[5]Centre for Polar Observation and Modelling, Department of Space and Climate Physics, University College London, London, England, United Kingdom.
[6]Institute of Scientific Instruments, Uzbekistan Academy of Sciences, Tashkent, Uzbekistan.
[7]Arctic and Antarctic Research Institute, St. Petersburg, Russia.
[8]Alfred-Wegener-Institut für Polar- und Meeresforschung, Bremerhaven, Germany.

0148-0227/02/2000JB000129$09.00

Figure 1. Map of Severnaya Zemlya showing the Academy of Sciences Ice Cap on Komsomolets Island together with the other ice caps in the archipelago. Inset is the location of Severnaya Zemlya and the nearby Russian Arctic archipelagos of Franz Josef Land and Novaya Zemlya within the Eurasian High Arctic.

derived from synthetic aperture radar (SAR) interferometry to investigate ice flow.

2. Glaciological Background

[4] Approximately 50% of the 36,800-km^2 archipelago of Severnaya Zemlya is ice covered [*Dowdeswell et al.*, 2001; *Kotlyakov*, 2001]. Mean annual temperatures in Severnaya Zemlya are about −16°C, compared with about −12°C in Franz Josef Land and −9°C in Novaya Zemlya (Figure 1) [*Dowdeswell*, 1995]. Precipitation increases from ∼0.25 to 0.45 m yr^{-1} (water equivalent) between sea level and the summits of the major ice caps [*Bryazgin and Yunak*, 1988]. The equilibrium line altitude on the ice caps of the archipelago varies between in excess of 600 m above sea level in the southeast, through ∼300 m on the Academy of Sciences Ice Cap, to 200 m or less on Schmidt Island in the northwest [*Govorukha*, 1970], suggesting a predominant moisture source and precipitation gradient from the north (Figure 1). Mass balance data are available only for a single site at the crest of the Academy of Sciences Ice Cap. However, mass balance measurements for the Vavilov Ice Cap [*Barkov et al.*, 1992], a 1,820-km^2 ice cap on October Revolution Island some 120 km to the south (Figure 1), indicate that the mean net balance was slightly negative between 1974 and 1988 (−0.03 m yr^{-1} water equivalent),

although there was a high interannual variability (standard deviation ±0.36 m yr^{-1}), making the mean indistinguishable from zero. Mean annual temperature in the archipelago is about −16.5°C and mean July temperature is about 1°C [*Bryazgin and Yunak*, 1988]. Total precipitation, both solid and liquid, is measured as an average of between 220 and 270 mm yr^{-1} at coastal stations in the archipelago and at 410 mm yr^{-1} on the Vavilov Ice Cap [*Bryazgin and Yunak*, 1988]. *Bryazgin and Yunak* [1988] estimate solid precipitation on the summit of Vavilov Ice Cap as between 250 and 300 mm yr^{-1}.

[5] Previous glaciological investigations on the Academy of Sciences Ice Cap have been undertaken by scientists from the former Soviet Union. Airborne radio echo sounding measurements have been made at a frequency of 100 MHz [*Bogorodskiy and Fedorov*, 1971; *Bogorodskiy et al.*, 1985], but the production of accurate digital elevation models of ice surface, thickness, and bedrock was difficult because of limited coverage and poor navigational accuracy during flying. Deep ice cores were also collected by Soviet scientists from both the Academy of Sciences Ice Cap and the Vavilov Ice Cap on October Revolution Island (Figure 1). The oxygen isotope and melt layer records in these ice cores (760 and 550 m) indicate that temperatures have risen markedly in the last 120–140 years in Severnaya Zemlya [*Vaikmyae and Punning*, 1982; *Kotlyakov et al.*, 1989, 1990], but interpretation of the older parts of each core is hampered by poor chronological control associated with the effects of surface melting on isotope and chemical stratigraphy [*Tarussov*, 1992].

[6] Aerial photographs of the archipelago, acquired since the 1930s, have been interpreted to record a general retreat of glacier margins, linked to the termination of the Little Ice Age, as indicated in the ice core record. A loss of ~500 km^2 of ice-covered area in Severnaya Zemlya is reported between 1931–1984 [*Govorukha et al.*, 1987], although *Koryakin* [1986] suggests that this may be an overestimate resulting from errors in aerial photograph interpretation.

Table 1. System Parameters of the 100-MHz Radar Used in Severnaya Zemlya

Parameter	Value
Center frequency	100 MHz
Transmitter pulse length	0.35 or 1.1 μs
Transmitter peak pulse power	250 or 1000 W
Transmitter pulse rate	10 kHz
Receiver bandwidth[a]	30 or 3 MHz
Receiver noise	6 dB
System performance (excluding antenna gain)	150 dB (short pulse), 160 dB (long pulse)

[a] Receiver type is successive detection log amplifier.

3. Methods

3.1. Airborne Radar Investigations

[7] For our 1997 airborne radar program in Severnaya Zemlya a new radar and antenna system, operating at a frequency of 100 MHz, was fabricated. The specifications of the radar system are given in Table 1. The antennae for the system were of three-element quad type, with one for transmitting and a second for receiving. The antennae were mounted on either side of a helicopter fuselage. Antenna gain (one-way) was 11 dB over isotropic. A digital data acquisition system recorded data simultaneously with an analogue photographic backup system. The digital system employed a fast digitizer to record complete waveforms (at a 50-ns digitizing interval), allowing the recovery of absolute power levels

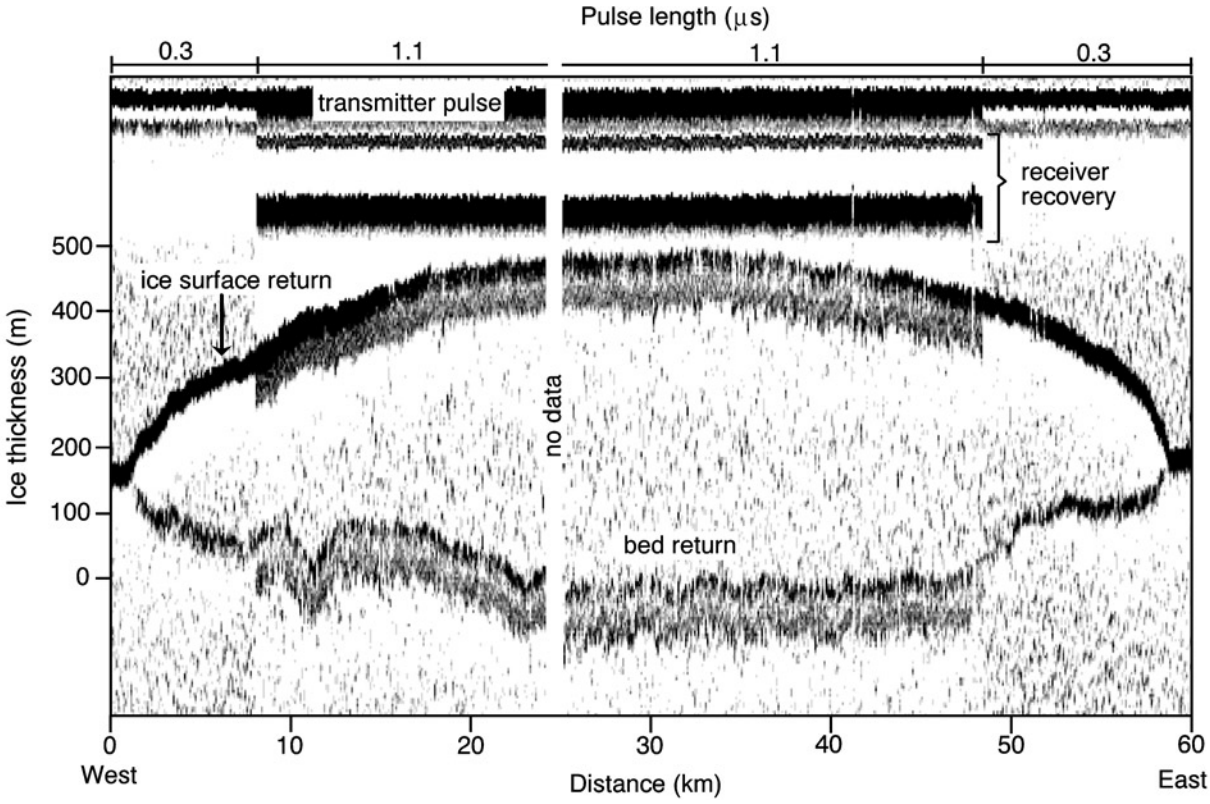

Figure 2. Radio echo sounding data from a flight track across the northern part of the Academy of Sciences Ice Cap (bold line in Figure 3). Note the differing surface and bed returns resulting from the use of the long- and short-pulse modes (1.1 and 0.35 μs, respectively) on the 100-MHz radar system (Table 1).

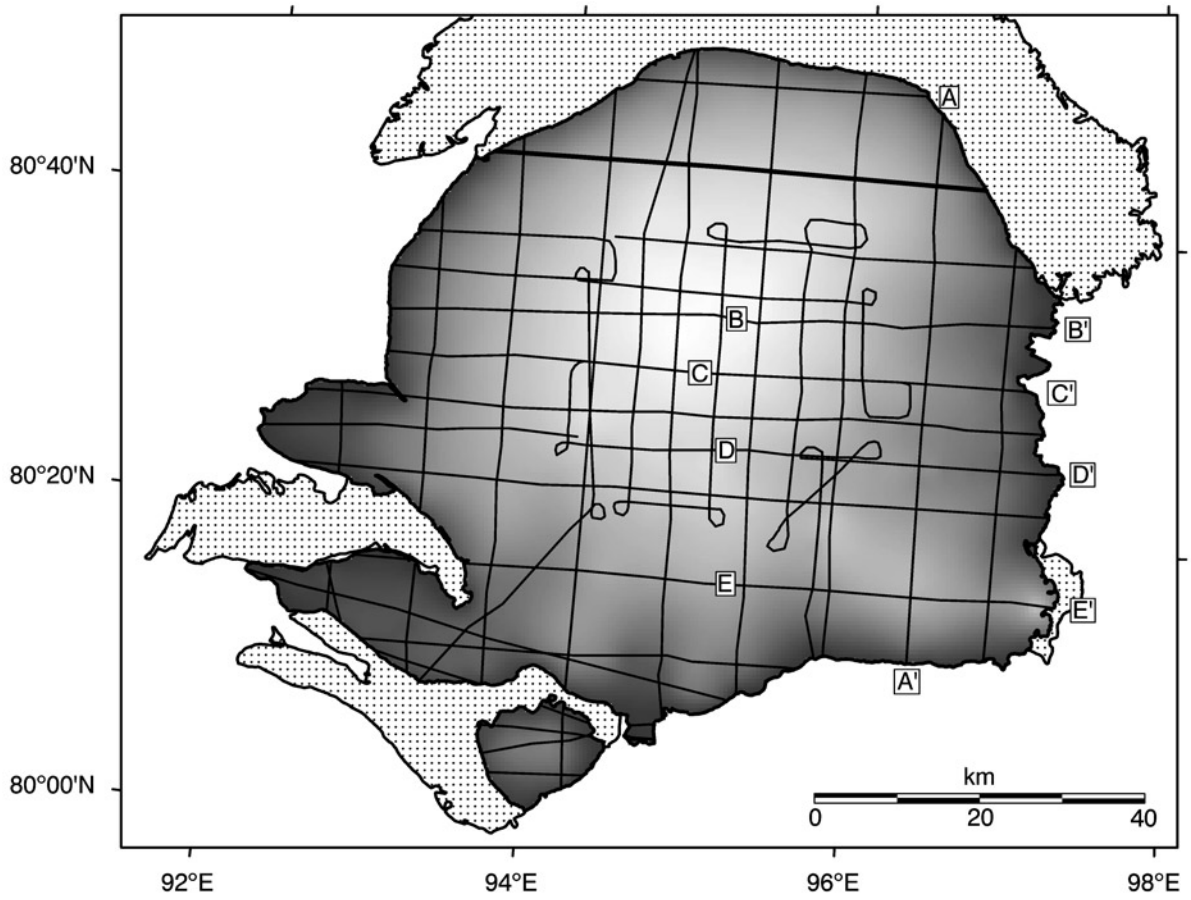

Figure 3. Map of airborne radio echo sounding flight paths on the Academy of Sciences Ice Cap (shaded area). The bold flight path line on the northern part of the ice cap is the radio echo record illustrated in Figure 2. Flight paths labeled A–A′, B–B′, C–C′, D–D′, and E–E′ are illustrated as reduced ice surface and bed profiles in Figure 8. The dotted areas denote bare land.

and power reflection coefficients. An example of a digital radar record across the ice cap is given in Figure 2. The analogue system recorded on film an intensity-modulated representation of echo time delay against distance along the flight track. This so-called "*Z*" mode display provided immediately accessible ice thickness data but only a qualitative indication of echo strength.

[8] The program of airborne radio echo sounding of the ice caps on Severnaya Zemlya took place between April 3 and May 7, 1997. Scientific flying was undertaken from a Russian MI-8MT helicopter, operated from the Russian base on Middle (Sredniy) Island, Severnaya Zemlya, throughout the scientific program (Figure 1). The helicopter flights were at a nominal air speed of 180 km hr^{-1} and were flown at a constant pressure altitude which ranged from 700 to 1,100 m, depending on weather conditions. A series of five scientific flights of up to 5.75-hour duration was undertaken on the Academy of Sciences Ice Cap. On each flight a significant amount of time was required for positioning legs over land or water. Dedicated flights were also made for equipment testing after installation and for over-water calibration of the radio echo sounding system. To locate the helicopter position and altitude, GPS positions and pressure altimeter data were recorded.

[9] A map of the flight lines over the Academy of Sciences Ice Cap is given in Figure 3. The ice cap was covered by a 10-km-spaced grid of flight paths, and the central portion was covered by a grid at 5-km intervals (Figure 3). Several additional lines were also acquired from flow lines down specific outlet glaciers that were unsuitable for coverage by the gridding scheme. A total of 1,657 km of radar data was obtained over the Academy of Sciences Ice Cap (Figure 3).

[10] The digital radar data were analyzed by plotting the differentiated waveforms of returned power in *Z* mode. The first surface and bed return for each waveform was then identified using a tracking algorithm [*Cooper*, 1987]. To check that the algorithm was tracking the correct interface, the tracked surface and bed returns were superimposed on the raw *Z* mode display (Figure 2). Sections of flight track with particularly weak or intermittent bed returns were tracked manually. Internal layering was not observed in the records. Absolute aircraft altitudes were calculated by calibrating pressure-altimeter measurements over the sea surface adjacent to the ice cap. Ice surface elevations were then derived by subtracting helicopter terrain clearance measured by the radar from the absolute altitude of the helicopter.

[11] Analysis of the differences in measured ice surface elevation and ice thickness at points where flight tracks crossed was used to assess the accuracy and consistency of the measurements. The distribution of measurement errors was not random over the ice cap. Larger errors in ice surface elevation, with a maximum of 16 m, were generally distributed around the steeper margins of the ice cap. The mean difference in ice surface elevation measurements at the 90 crossing points was 6.9 m, with a standard deviation of 4.9 m.

[12] The largest crossing point errors in the measurements of ice thickness were concentrated near the center of the ice cap, where radio echo returns from the ice cap bed were weakest because of greater absorption of electromagnetic energy along a longer two-way path length and because of scattering by ice inclusions within

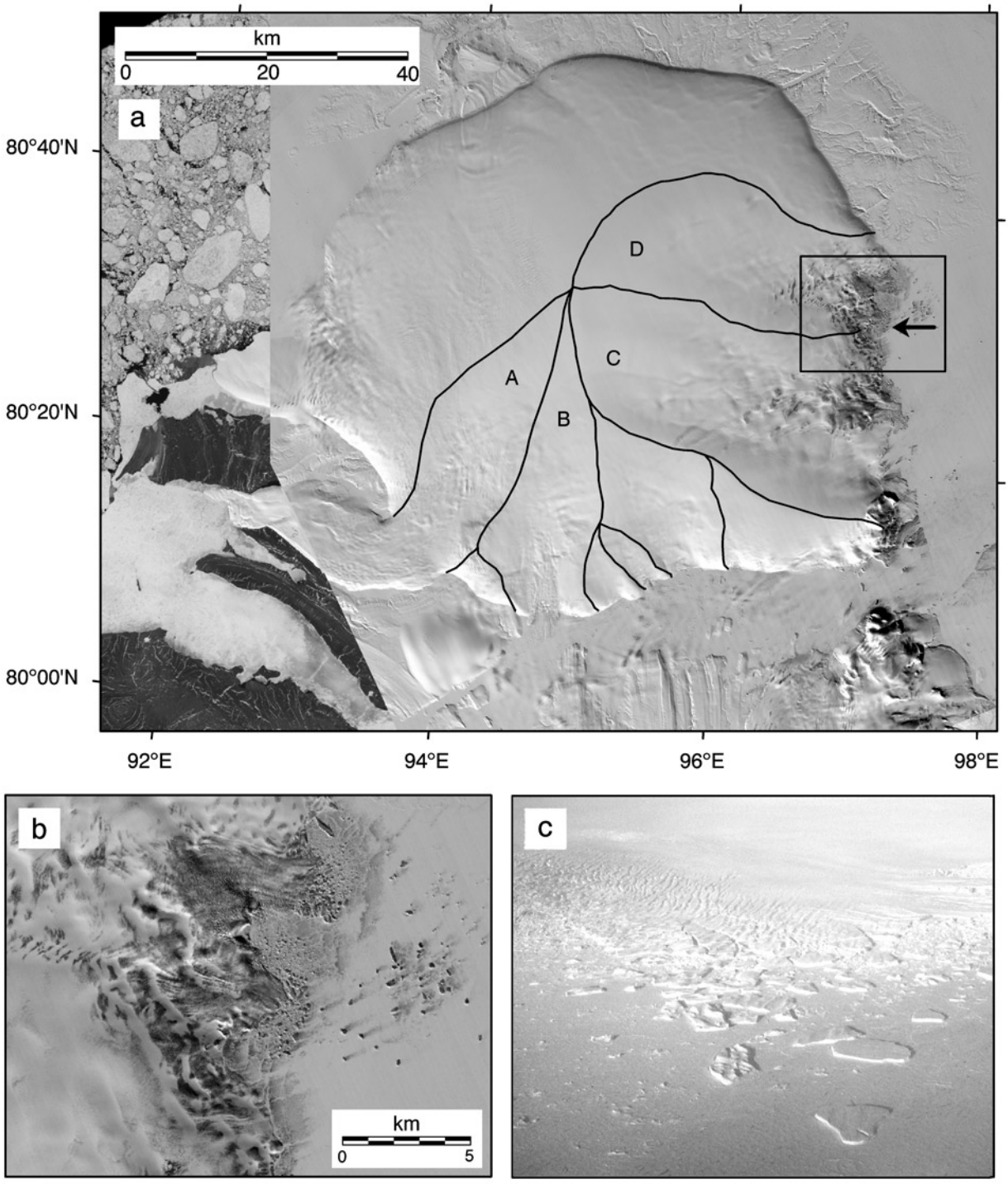

Figure 4. (a) Mozaic of two Landsat images of the Academy of Sciences Ice Cap, Severnaya Zemlya, showing the ice divides defining the drainage basins (labeled A, B, C, and D) of four ice-stream-like features (informally named ice streams 1, 2, 3, and 4, repectively). Landsat images are thematic mapper path/row 174/001 acquired on April 26, 1988 (east of 93°E) and multispectral scanner path/row 171/001 acquired on August 27, 1988. (b) An enlargement of part of the spring 1988 Landsat image (outlined by the box in Figure 4a), showing tabular icebergs calving from an ice stream margin on the eastern side of the ice cap and trapped in shorefast sea ice. (c) Oblique aerial photograph of tabular icebergs calving from a heavily crevassed ice-stream-like feature on the eastern side of the ice cap (approximate viewing direction indicated by the arrow in Figure 4a). The photograph was taken in April 1997, and the sea surface was covered with shorefast sea ice at this time.

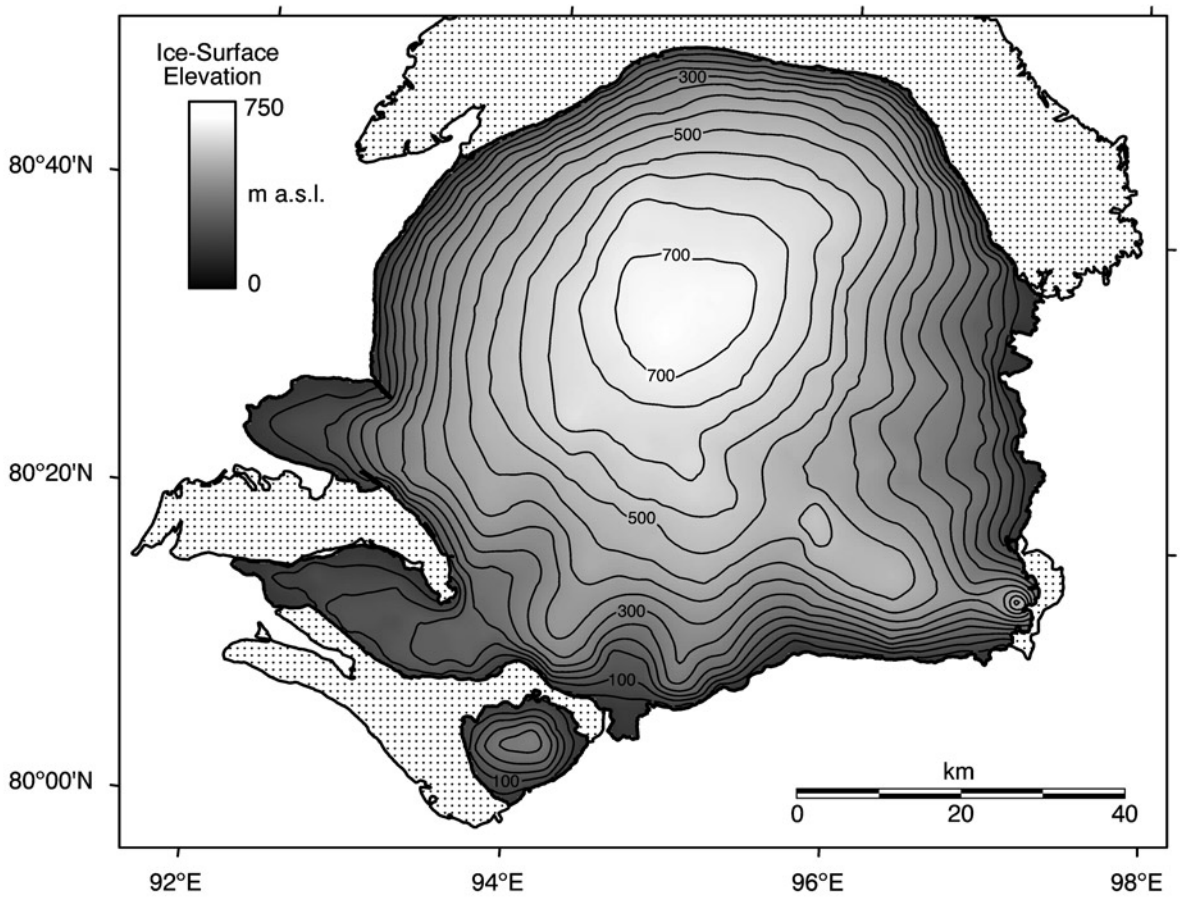

Figure 5. Surface topography of the Academy of Sciences Ice Cap, Severnaya Zemlya, derived from airborne altimetric data (Figure 3). Contours are at 50-m intervals. Dotted areas denote bare land.

firn of the accumulation zone. The mean crossing point error in ice thickness measurements was 10.5 m, or 2.4%, of ice thickness, with a standard deviation of 7.6 m, or 1.7%.

[13] Our reduced radar measurements of ice surface elevation and ice thickness along flight paths were then interpolated over the whole ice cap using ordinary kriging with prior semivariogram analysis [*Isaaks and Srivastava*, 1989]. This method was adopted because kriging is an optimal interpolator of irregularly spaced point data. Gridded ice surface elevation and ice thickness data sets were produced with a cell size of 500 by 500 m. A digital terrain model of the ice cap bed was then derived by subtraction of ice thickness from surface elevation for each grid cell.

3.2. Satellite Remote Sensing

[14] Landsat thematic mapper (TM) and multispectral scanner digital imagery (Figure 4) with a spatial resolution of 30 m and 79 m, respectively, was used for three purposes during our studies of the Academy of Sciences Ice Cap. First, Landsat imagery was used to map the margins of the ice cap, after georeferencing to ground control points. Second, the qualitative topography of the ice cap surface, including the location of ice divides defining ice cap drainage basins, was derived from digitally enhanced Landsat pixel brightness values [e.g., *Martin and Sanderson*, 1980; *Dowdeswell et al.*, 1995]. This surface topographic information was used in the planning of helicopter flight paths for radio echo sounding. Third, Landsat imagery was also examined for the presence of indicators of surge behavior on both the Academy of Sciences Ice Cap and, more generally, over the whole archipelago. Ice surface features, including looped medial moraines and heavy surface crevassing, together with rapid changes in ice extent [e.g., *Meier and Post*, 1969; *Liestøl*, 1993], relatively easily observed on summer Landsat imagery, have been used to identify any possible surge activity within the outlet glaciers of the Academy of Sciences Ice Cap [*Dowdeswell and Williams*, 1997].

[15] Satellite radar interferometry was used to calculate the velocity structure of the Academy of Sciences Ice Cap. Very few velocity measurements of the ice caps on Severnaya Zemlya were available through traditional ground survey methods, and there are no data on velocity gradients and change through time, which are important parameters in understanding the dynamics of nonsteady glacier flow. The interferograms are derived from pairs of ERS-1/ERS-2 SAR images, obtained from satellite passes one day apart in September and December 1995, that are registered using a correlation algorithm. The phase difference in an interferogram is a result of range change between two satellite passes, where range is affected by both horizontal and vertical ice displacement, as well as by the interferometric baseline between passes. The effects of ice surface topography are removed by subtracting a synthetic interferogram generated from our digital elevation model [*Massonnet et al.*, 1993]. Errors in interferometric baseline estimates can also introduce a quasi-linear phase ramp of several fringes across an image [*Joughin et al.*, 1996]. This ramp has been removed using tie points from areas of bare land [*Zebker et al.*, 1994], where displacement should be zero, together with a series of topographic tie points from our digital terrain model derived from airborne ice surface altimetric data.

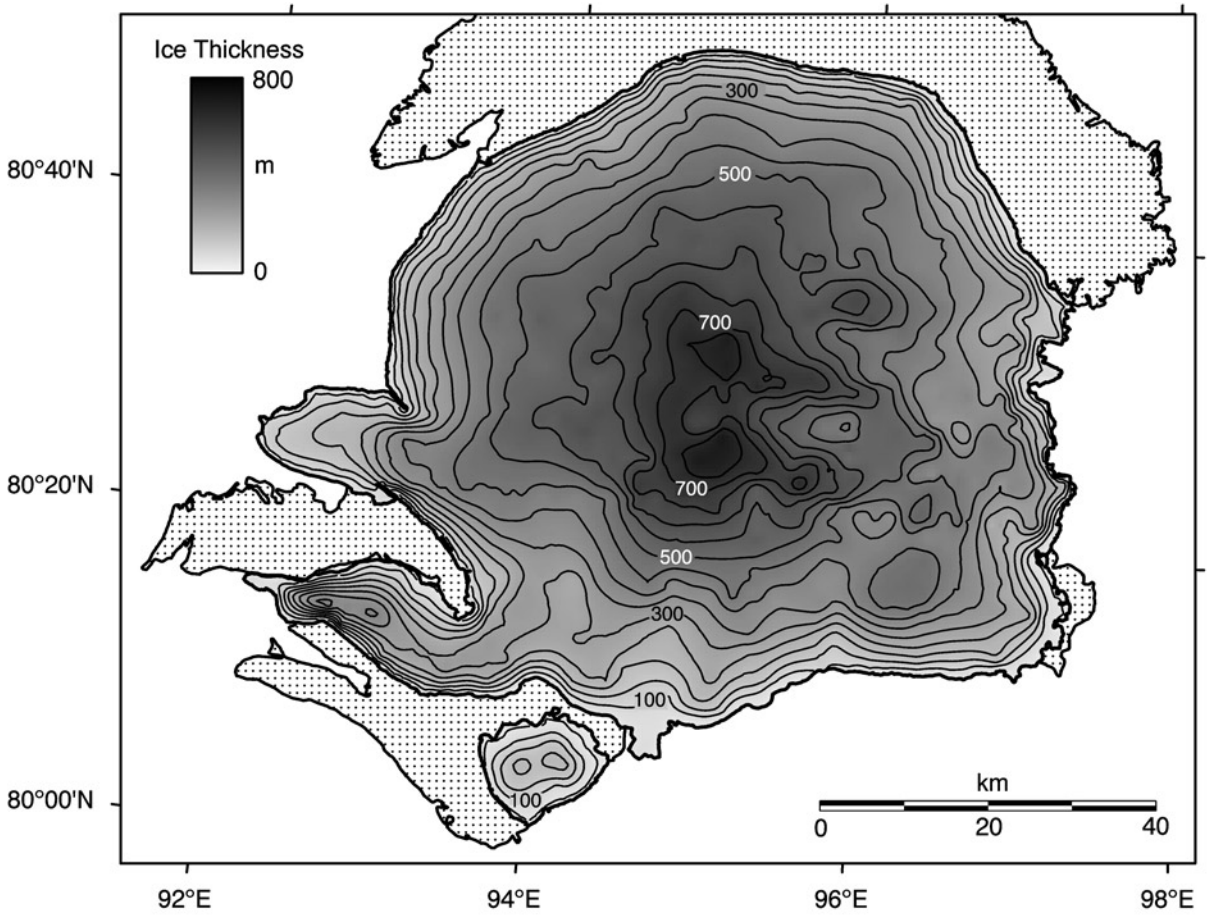

Figure 6. Thickness of the ice of the Academy of Sciences Ice Cap, Severnaya Zemlya, derived from airborne radio echo sounding data (Figure 3). Contours are at 50-m intervals.

[16] Interferograms of the Academy of Sciences Ice Cap were generated using the above methods and corrections. They can be viewed as contour maps of surface displacement in the satellite viewing direction, with each fringe (i.e., cycle of the color wheel) representing a change of 15 m yr^{-1}. The errors in the velocity estimates, which are dependent on the interferometric baseline, were 0.3 m yr^{-1} and 1.8 m yr^{-1} for the September and December 1995 interferograms, respectively, of the ice cap. Coherent interferometric fringes were produced over almost the whole 5,575-km^2 ice cap. These data were phase unwrapped and then used to produce ice surface velocities in the look direction of the SAR and, on the assumption that ice flow is greatest in the direction of maximum ice surface slope, to produce a corrected velocity field (v_{corr}).

4. Airborne Radar Results: Ice Cap Morphology and Thickness

4.1. Ice Surface Morphology

[17] The surface topography of the Academy of Sciences Ice Cap is relatively simple. A digital terrain model of the ice surface, produced from our airborne radar data, is shown in Figure 5. The ice cap consists of a single well-defined dome, whose crest rises to an elevation of 749 m. The dome is displaced to the north of the geographical center of the ice cap. As a result of this, the gradient of the ice surface is steeper to the north than to the south on the ice cap. There is also a ridge trending southeast from the main dome, which contains a small subsidiary summit (Figure 5).

[18] The northern and northwestern parts of the ice cap are relatively uniform in surface slope, whereas the southern and eastern ice cap margins are dissected by several troughs in the ice surface separated by ice ridges (Figure 5). Inspection of Landsat satellite imagery shows that these troughs contain ice that appears rough at a kilometer scale and whose margins are relatively well-defined (Figure 4a). Crevasses can be resolved in some cases (Figure 4b). These features are morphologically similar to ice streams reported from other Arctic ice caps [e.g., *Dowdeswell and McIntyre*, 1987; *Dowdeswell and Collin*, 1990] and from the West Antarctic Ice Sheet [e.g., *Bentley*, 1987]. The ice-stream-like features on the Academy of Sciences Ice Cap are identified on the Landsat image shown in Figure 4a.

[19] Ice divides, marking the boundaries of ice cap drainage basins, are also identified on Landsat imagery (Figure 4a). These divides are more easily defined on the southern and eastern sides of the ice cap, where ice flow appears relatively variable between surface topographic valleys and ridges, than on the northern and northwestern slopes, where the ice surface appears more uniform in morphology.

[20] The Academy of Sciences Ice Cap terminates partly on land and partly in the marine waters of the Kara and Laptev Seas, to the west and east, respectively, of Severnaya Zemlya (Figure 1). About 200 km, or 42%, of the ice margin is marine, located on the northwest, south, and east sides of the ice cap. The main areas where the ice cap ends on land are to the north and southwest (Figure 5). Radar records and visual observations show that the marine margins of the ice cap are marked by terminal ice cliffs, whereas the ice surface on land slopes smoothly to the ice edge. Icebergs, some of which are tabular and up to ~1.7 km in length, are imaged on Landsat scenes (Figure 4b) and were also observed

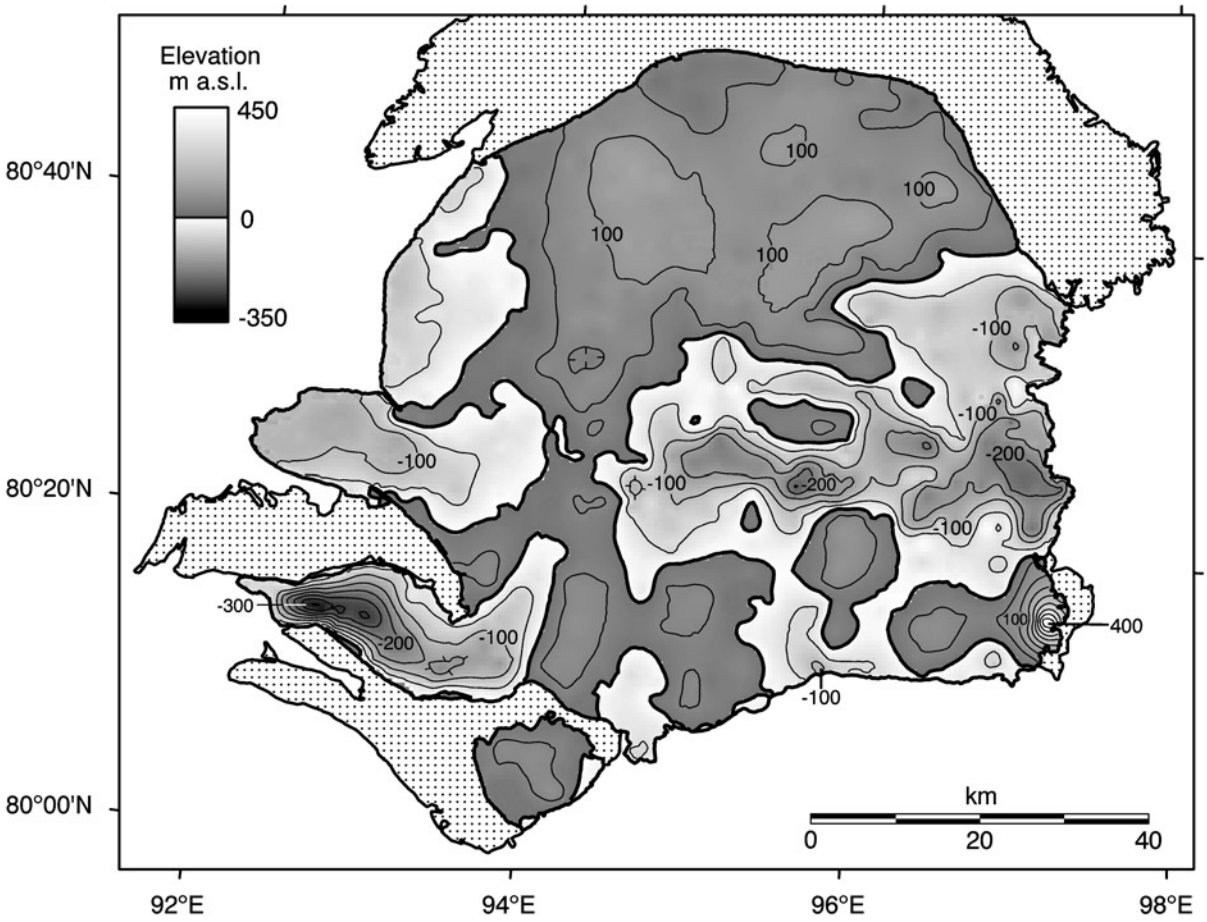

Figure 7. Topography of the bed of the Academy of Sciences Ice Cap, Severnaya Zemlya, derived from airborne radio echo sounding data (Figure 3). Contours are at 50-m intervals. The bold contours represent sea level (i.e., 0 m of elevation).

on helicopter flights during the acquisition of radar data. These icebergs are concentrated particularly at the margins of the ice-stream-like features on the eastern and southern margins of the ice cap (Figure 4c).

[21] To the southwest of the Academy of Sciences Ice Cap on Komsomolets Island is the 133-km^2 Separate (Otdelniy) Ice Cap (Figure 5). Comparison of Russian maps, based on aerial photographs acquired during the 1950s, with recent Landsat satellite imagery indicates that this small ice cap was formerly attached to the main dome but is now separated by a 5-km-wide belt of land. The surface topography of Separate Ice Cap is also mapped from our radar data (Figure 5). The highest point on this small ice cap is measured at 282 m.

4.2. Ice Thickness and Bed Elevations

[22] A digital terrain model of the thickness of the Academy of Sciences Ice Cap, derived from our 100-MHz radar data, is illustrated in Figure 6. Using the digital terrain model of ice thickness, a total ice volume of 2,184 km^3 is calculated. This is equivalent to ~5.5 mm of sea level rise, were the entire ice cap to melt: a process that could take on the order of 10^3 years.

[23] Ice thickness generally increases fairly monotonically from the ice cap margins to its center, with the most rapid increases in thickness occurring close to the ice edge. There is a clear, and expected, positive relationship between ice thickness gradient and ice surface gradient. The thickest ice is located in two regions close to the ice cap center, with the maximum ice thickness reaching 819 m at the more southerly of these two areas (Figure 6). Ice thickness is most variable on the eastern side of the ice cap.

[24] The absolute elevation of the ice cap bed is shown as a contoured digital terrain model in Figure 7. About 50% of the bed is below present sea level, and long profiles of the ice cap show that parts of its bed lie below sea level over 40 km inland of the ice margin (Figure 8). The minimum bed elevation is −207 m on the eastern side of the ice cap and about −317 m in the southwest. There is a clearly defined subglacial valley running east-west beneath the ice cap, with a particularly deep trough on the eastern side (Figures 7 and 8). The northern part of the ice cap is, by contrast, underlain by a relatively smooth topography that is above modern sea level.

[25] It should be noted that the ice-stream-like features identified in ice surface elevations and Landsat imagery are located in troughs within eastern and southern parts of the ice cap bed (Figure 7). Ice surface and bed profiles, located both along and across flow lines down these features and the intervening ice surface ridges, illustrate this clearly (Figure 8). The locations of these ice-stream-like features therefore appear to be influenced strongly by bed topography. The subglacial troughs tend to increase in depth toward the ice cap margins. Subglacial troughs are also present at two locations on the northwestern side of the ice cap (Figure 7). These troughs are not, however, filled by well-defined ice-stream-like features. Instead, ice with a much smoother surface character is present (Figure 4a), suggesting that the northwestern margin of the ice cap is different dynamically from that of the south and east.

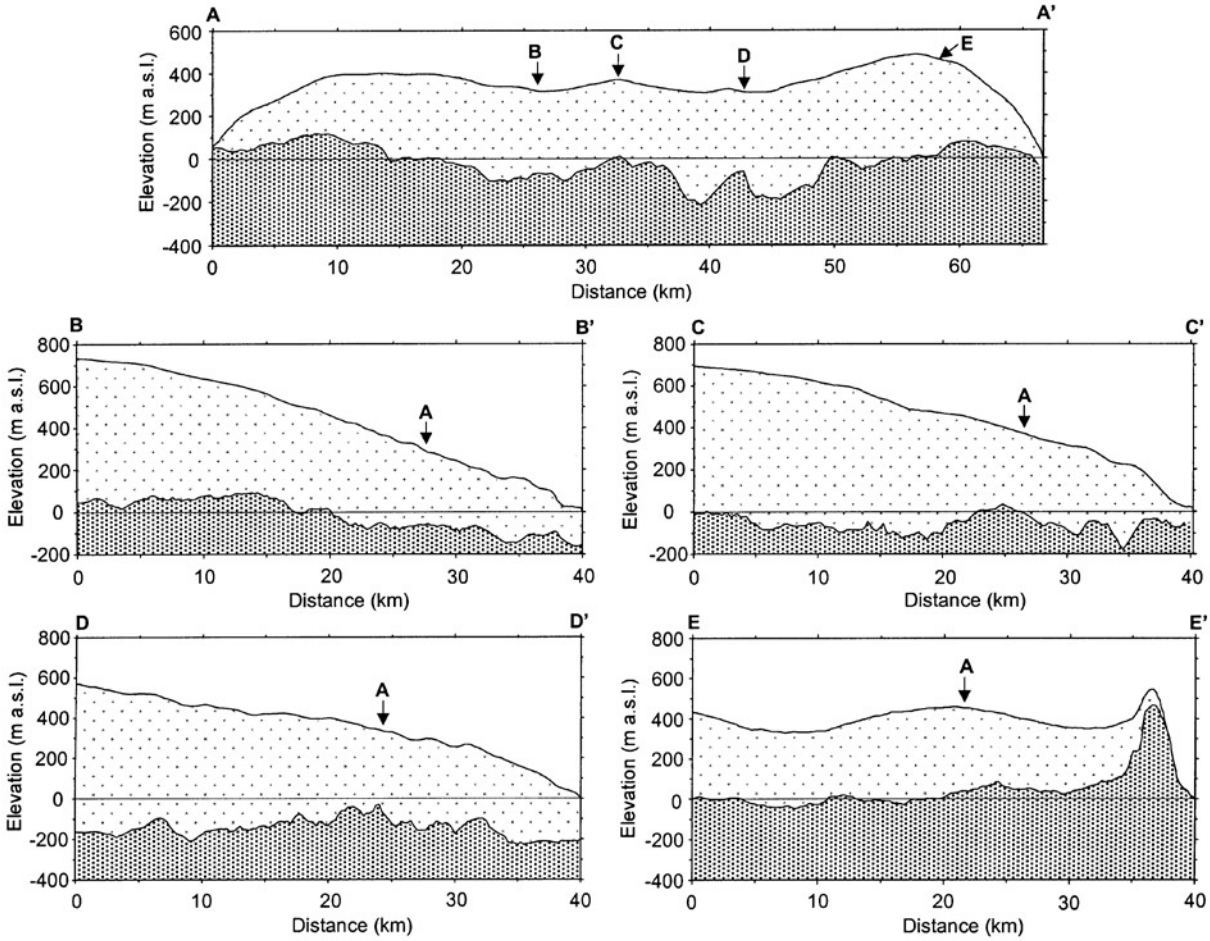

Figure 8. Long and cross profiles of the ice surface and bed topography of the eastern side of the Academy of Sciences Ice Cap (profiles located in Figure 3). Note that the cross profile A–A′ shows the two ice-stream-like features and the intervening ridge.

[26] There is some evidence from both our radar work and earlier investigations by Russian scientists that parts of the ice cap margin at the seaward end of the ice streams may be floating. First, earlier Russian work identified an area of ~10 km^2 on the north-eastern margin of the ice cap as having a very low ice surface profile. This was interpreted as evidence for a floating ice shelf [*Zinger and Koryakin*, 1965; *Dowdeswell et al.*, 1994]. Second, we observed both very low ice surface gradients and particularly strong radar returns from the ice-cap bed in several areas at the margin of the ice-stream-like features. Third, large numbers of tabular icebergs were observed at the margins of these features (Figure 4) and are interpreted qualitatively to indicate that the calving margins are buoyant or approaching this state.

[27] Our 100-MHz airborne radar system acquired returns from the ice cap bed over more than 97% of flight tracks. Bed returns were occasionally absent in two settings. First, in a few areas, mainly close to terminal ice cliffs and in some parts of the ice-stream-like features where many crevasses were present, bed returns were sometimes difficult to distinguish within noise from internal scattering of the radar signal. Second, bed returns were weaker beneath the thickest ice at the center of the ice cap, presumably due to a combination of absorption on increasingly long two-way travel paths and to scattering from ice inclusions within the firn of the accumulation area [*Smith and Evans*, 1972]. The entire radar survey was conducted before the start of the melt season, and there is therefore no effect from meltwater within the snowpack.

5. Dynamics of the Academy of Sciences Ice Cap

5.1. Inferences from Landsat Digital Imagery

[28] Landsat images reveal the major ice divides of the Academy of Sciences Ice Cap, particularly after digital contrast stretching (Figure 4a). The central divide of the ice cap and several major drainage basins, in the south and east of the ice cap and of up to 975 km^2, are delimited from the satellite imagery. However, the very smooth ice surface in the north and northwest of the ice cap implies that ice flow is very uniform and undifferentiated in these areas. Each of the five largest drainage basins identified on the ice cap has surface topography that appears rough at a kilometer scale on Landsat imagery (Figure 4a).

[29] Landsat imagery acquired in both spring and summer conditions was also examined for evidence of any deformation of either large-scale ice structures or medial moraines [*Meier and Post*, 1969; *Hambrey and Dowdeswell*, 1994]. Neither medial moraines were present on the Academy of Sciences Ice Cap, nor were any ice structures indicative of deformation observed. There is therefore no evidence of past surge activity on the ice cap within the residence time of the ice. This appears to be typical of the ice

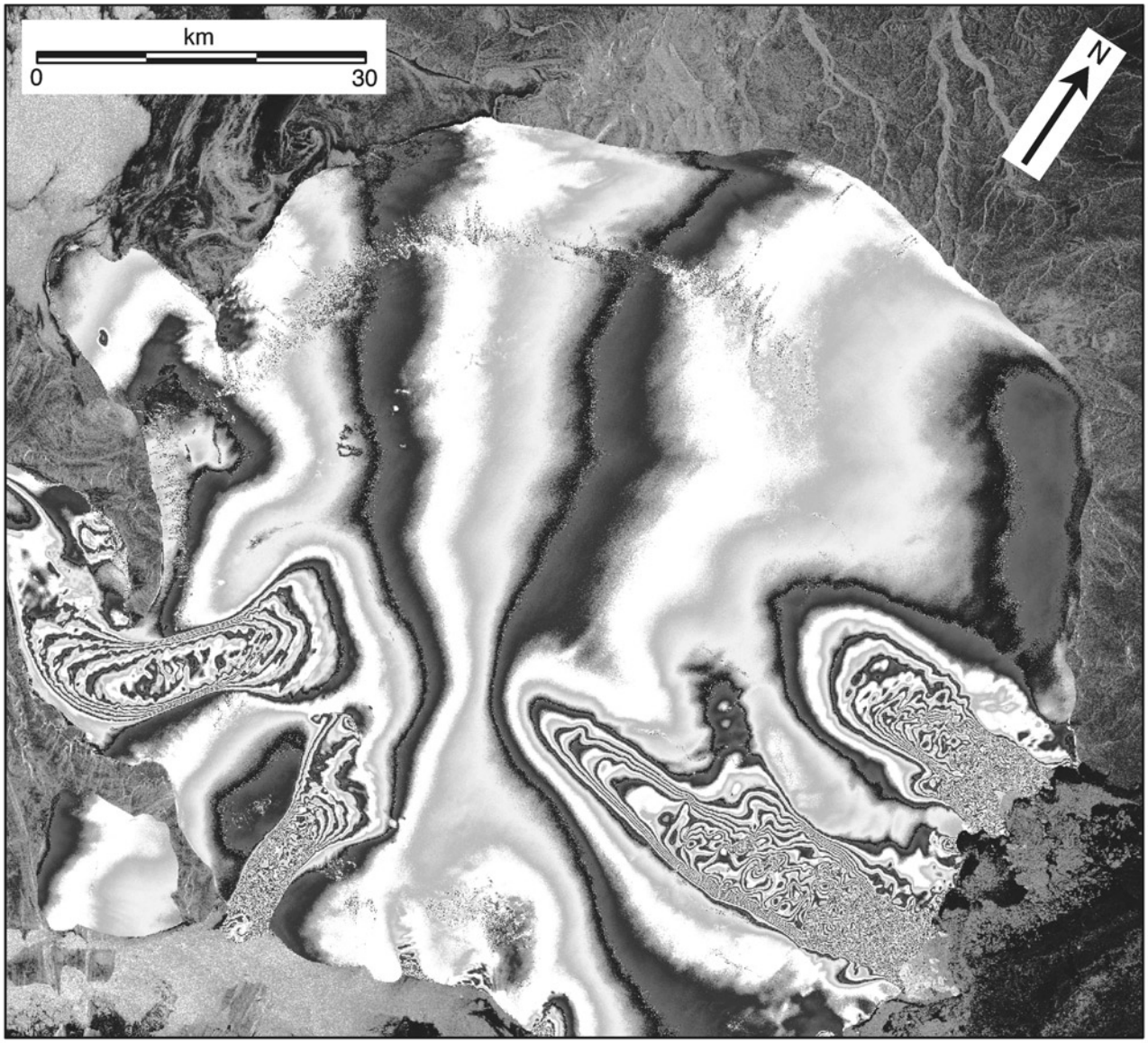

Figure 9. Synthetic aperture radar (SAR) interferorgram of the Academy of Sciences Ice Cap in the slant range geometry of the ERS satellite. The pair of SAR images were acquired on September 23 and 24, 1995, during the ERS tandem phase. The interferometric parallel baseline between the two satellite locations is 1 m. The ramp across the interferogram has been removed during subsequent processing. The interferogram of the ice cap is superimposed on a Landsat image of the surrounding terrain and marine waters. See color version of this figure at back of this issue.

masses of the Russian Arctic archipelagos, where, in contrast with Svalbard [*Dowdeswell et al.*, 1991; *Liestøl*, 1993], only a very small number of glaciers show evidence of past surge activity [*Dowdeswell and Williams*, 1997].

5.2. Velocity Structure From SAR Interferometry

[30] Interferograms of the Academy of Sciences Ice Cap were derived from pairs of ERS tandem phase SAR images (Figure 9). They define the spatial pattern of ice surface velocity on the ice cap in the look direction of the satellite (v_{look}). The interferograms are phase unwrapped and then corrected to absolute velocity (v_{corr}) (Figures 10) on the assumption that ice flow is in the direction of maximum ice surface slope. The dome-shaped crest of the ice cap has a very low ice surface velocity (Figures 10 and 11). Ice divides marking the main crest, and the 749-m summit, of the Academy of Sciences Ice Cap are expected from theory to have near-zero horizontal velocity. Ice divides plotted from independent, geometrically corrected Landsat images coincide closely with minima in the interferometric phase (Figure 4a).

[31] The interferometric evidence from the outer parts of the ice cap falls into two parts. The bulk of the marginal zone is typified by few interference fringes and implies low velocity (Figures 9 and 10). This marginal zone is punctuated by four units of faster flow, represented by more closely spaced fringes. These units are labeled A, B, C, and D on the velocity map in Figure 10 and correspond to four of the drainage basins with rough ice surface topography identified on Landsat imagery (Figure 4a). They are referred to informally as ice streams 1–4 in this paper. A fifth basin with rough topography, on the south side of the ice cap (Figure 4a), shows only limited evidence of fast flow (Figure 10).

[32] These fast flowing units, or ice streams, have a series of tightly spaced fringes at their lateral margins (Figure 9). The pattern of fringes obtained over the Academy of Sciences Ice Cap using interferometry also shows that several of the fast flowing

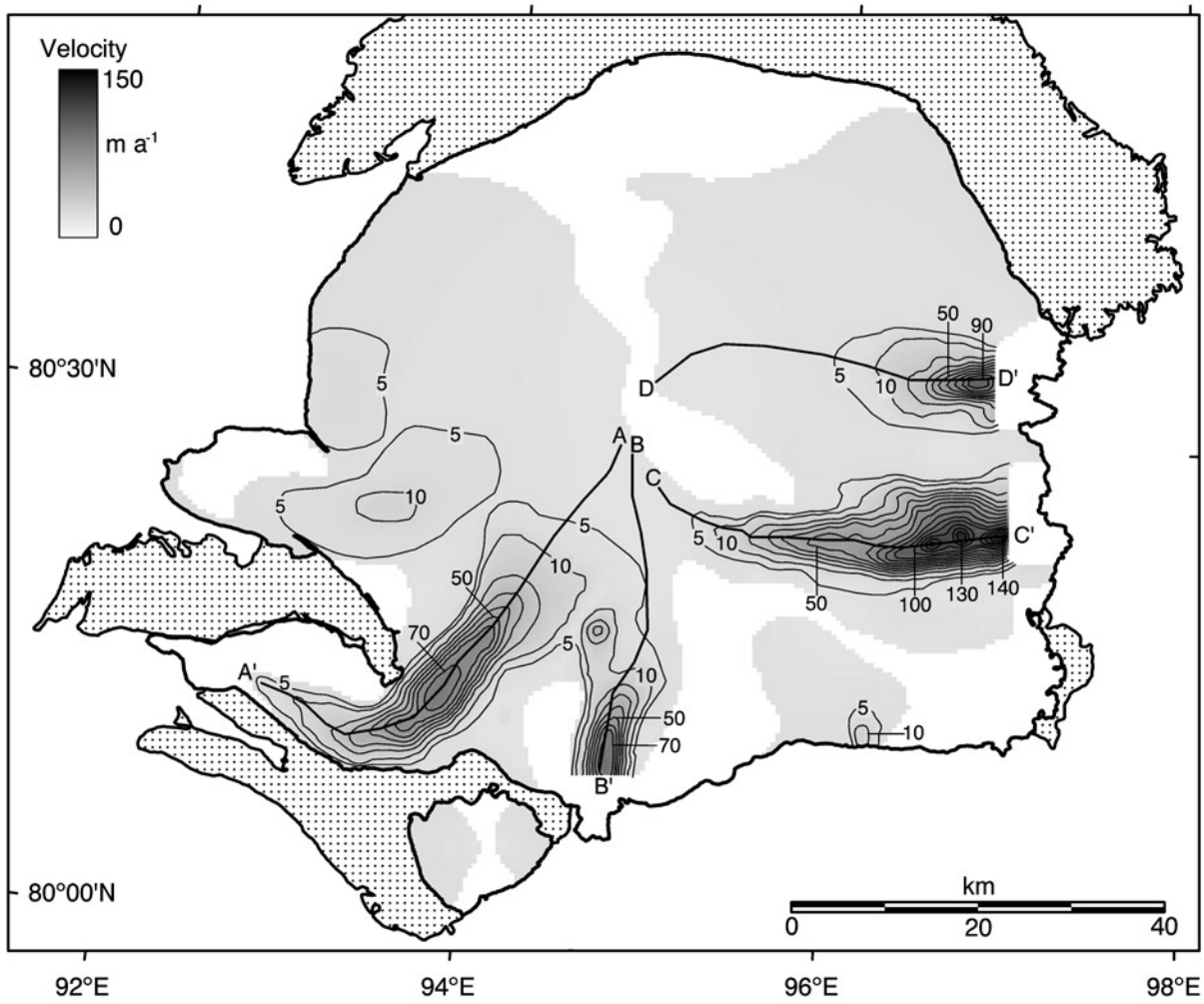

Figure 10. Corrected interferometrically derived ice surface velocities (v_{corr}) for the Academy of Sciences Ice Cap after phase unwrapping and the removal of topographic effects in the September 23–24, 1995, pair of ERS tandem phase scenes. The first two contours are at velocities of 5 and 10 m yr^{-1}, with subsequent contours at 10 m yr^{-1} intervals. Unshaded areas on the ice cap are regions of no v_{corr} data. A correction from viewing direction velocities (v_{look}) to velocity in the direction of maximum ice flow (assumed to be parallel to the angle of maximum ice surface slope) has been made. Dotted areas are bare land. Velocity profiles A–A′ to D–D′ on ice streams 1–4, respectively, are shown in Figure 11.

ice streams extend back into the generally slower moving ice to within 5–10 km of the central crest of the ice cap (Figures 9–11). This can be seen most clearly in the case of the more southern fast flowing unit on the east side of the ice cap.

[33] The four ice streams have lengths of between 17 and 37 km and widths of 4–8 km (Table 2). Ice streams 2, 3, and 4 appear to be similar in velocity structure (Figure 11). Their velocity gradient, expressed through the decreasing distance between interferometric fringes, increases toward the coastal ice margin, and phase coherence breaks down close to the terminus of each (Figure 9). This pattern of steadily increasing velocity within approach to the ocean (Figure 11) is typical of many tidewater outlet glaciers and ice streams in both the Antarctic and Arctic [e.g., *Bentley*, 1987; *Dowdeswell and Collin*, 1990]. These ice streams are the major locations of iceberg calving from the Academy of Sciences Ice Cap (Figures 4b and 4c).

[34] The fourth flow unit, ice stream 1, has a different velocity distribution. Velocity increases with relatively uniformity, reaches a plateau expressed in a closed interferometric fringe (Figure 9), and then decreases once more at a fairly uniform rate (Figure 10). The lowermost 12 km or so of this outlet glacier are of low velocity (Figure 11). This is a classical distribution of ice velocity, in which motion is greatest close to the equilibrium line [*Paterson*, 1994].

5.3. Mass Flux and Iceberg Production

[35] The mass flux through each of the fast flowing units can be calculated by combining our airborne observations on ice thickness (Figure 6), to yield fluxgates, with interferometrically derived velocity (Figure 10). The parameters for each of the four flow units are set out in Table 2. Comparison of the ice cap margins between SAR amplitude imagery from 1994 with earlier Landsat images from the 1980s shows that the ice front has changed position very little. Measurements of thickness and velocity close to the ice cap margins, which end in the ocean, therefore produce estimates of the flux of ice released as icebergs and thus specify this component of the mass balance of each drainage basin. Mass loss from ice streams 2, 3, and 4 ranges between 0.03 and 0.37 km^3 yr^{-1} (Table 2). Ice stream 1, however, has a very low rate of iceberg production, largely because the velocity of its lowermost few kilometers is very low (Figure 11). Its maximum flux is at ~25 km up-glacier, where mass transfer is ~0.1 km^3 yr^{-1}. At ice seaward margin, its flux is less than 0.02 km^3 yr^{-1}.

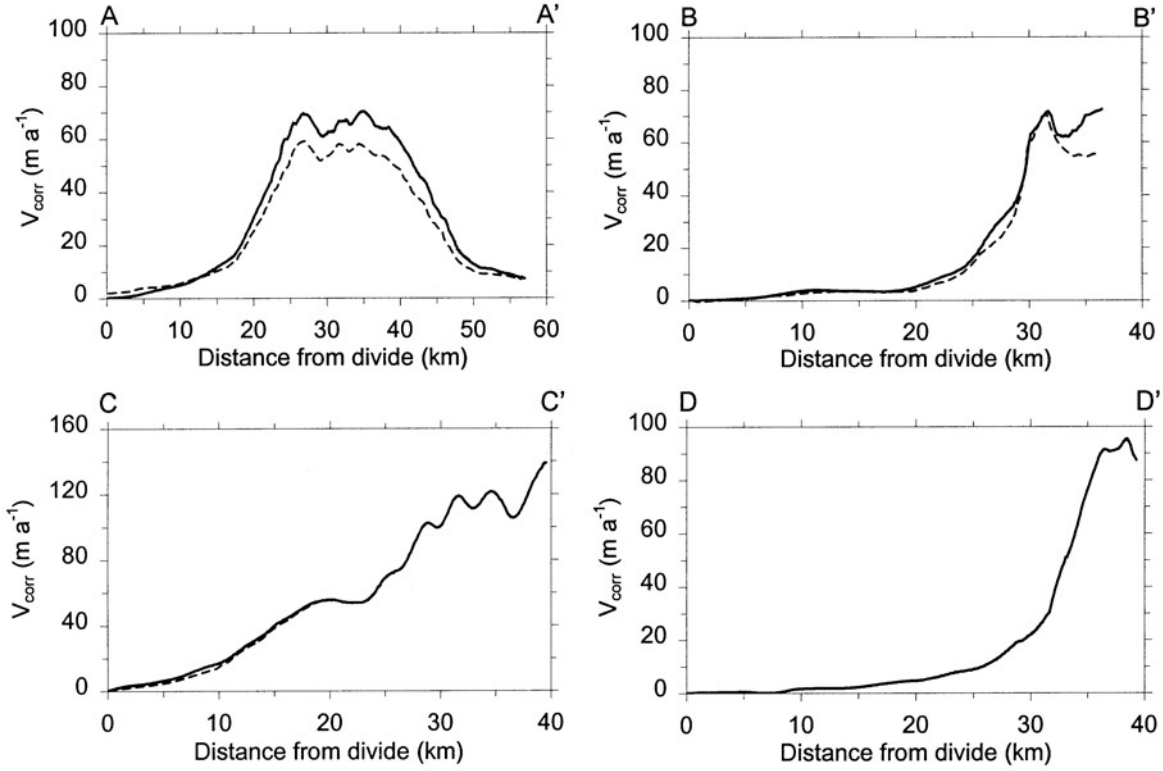

Figure 11. Velocity profiles (v_{corr}) along profiles down four fast flowing ice streams in the Academy of Sciences Ice Cap. The four profiles are located in Figure 10. The solid and dashed lines represent v_{corr} values for September 23–24, 1995, and December 2–3, 1995, interferometric pairs, respectively.

[36] The distribution of icebergs trapped in shorefast sea ice beyond the seaward margins of the Academy of Sciences Ice Cap has also been investigated from Landsat TM images acquired in April 1988 and June 1994. In each case, the images extend to the limit of the shorefast sea ice, ~50 km from the eastward margin of the ice cap, and the icebergs stand out clearly from the sea ice cover (Figure 4b). Icebergs are clustered about the fast flowing ice streams 2, 3, and 4, and their distribution extends outward into the sea ice. This distribution confirms that these ice streams (Figures 9 and 10) are the primary producers of icebergs from the ice cap.

[37] Summing the iceberg flux values from Table 2 yields a calving rate of 0.54 km^3 yr^{-1} for the four margins examined. These seaward margins of the ice cap represent 24 km, or 12%, of the total length of ice-ocean interface. Interferometrically derived velocities are less than 10 m yr^{-1}, and often less than 5 m yr^{-1}, around almost all of the remaining 176 km of this interface (Figure 10), implying a further iceberg flux of less than 0.1 km^3 yr^{-1}, assuming a 100-m thickness at the margin (Figure 6). Thus the total flux of icebergs from the Academy of Sciences Ice Cap is likely to be ~0.65 km^3 yr^{-1}.

[38] Iceberg production is one of two major components of the mass balance of the 5,575-km^2 ice cap. The other mechanism of mass loss is from surface melting. Basal melting of floating ice is probably negligible because floating ice at the margin covers no more than ~15 km^2 at most. The magnitude of basal melting beneath grounded ice is calculated simply as ~4 mm yr^{-1} [e.g., *Hooke*, 1998]. Even if this were taking place over the whole of the ice cap base, which is unlikely, the rate of mass loss would be several orders of magnitude less than losses through surface meltwater and iceberg production. Recent borehole measurements indicate a basal temperature of −8°C beneath the ice cap crest [*Fritzsche et al.*, 2001], and earlier Russian data also suggest negative temperatures [*Zagorodnov et al.*, 1989]. It is probable that basal melting is restricted to areas of relatively fast flowing ice (Figures 9 and 10).

[39] Measurements elsewhere in the Severnaya Zemlya archipelago suggest that annual precipitation may vary from 0.25 to 0.45 m yr^{-1} (in water equivalent) with altitude [*Bryazgin and Yunak*, 1988]. We know little about the surface mass balance of the Academy of Sciences Ice Cap. However, recent analyses of the

Table 2. Dimensions and Flow of Four Fast Flowing Ice Streams on the Academy of Sciences Ice Cap (Figure 9)

Ice Stream (Lines in Figure 10)	Basin Area, km^2	Length, km	Width, km	Thickness,[a] m	Velocity,[a] m yr^{-1}	Ice Flux,[b] km^3 yr^{-1}
1 (A–A′)	706	37	6	282	60	0.10[c]
2 (B–B′)	417	19	4	130	60	0.03
3 (C–C′)	975	33	8	390	120	0.37
4 (D–D′)	670	17	6	242	85	0.12

[a] Measurements (averaged across each ice stream) of ice thickness (from airborne radar) (Figure 6) and ice surface velocity (v_{corr} from SAR interferometry) (Figures 10 and 11) are from the marginal 5 km of the ice cap.
[b] Ice flux values represent measurements at the ice cap margins, except for ice stream 1 where measurements are taken from 25 km up-glacier.
[c] Flux at the margin of the ice stream is <0.02 km^3 yr^{-1}.

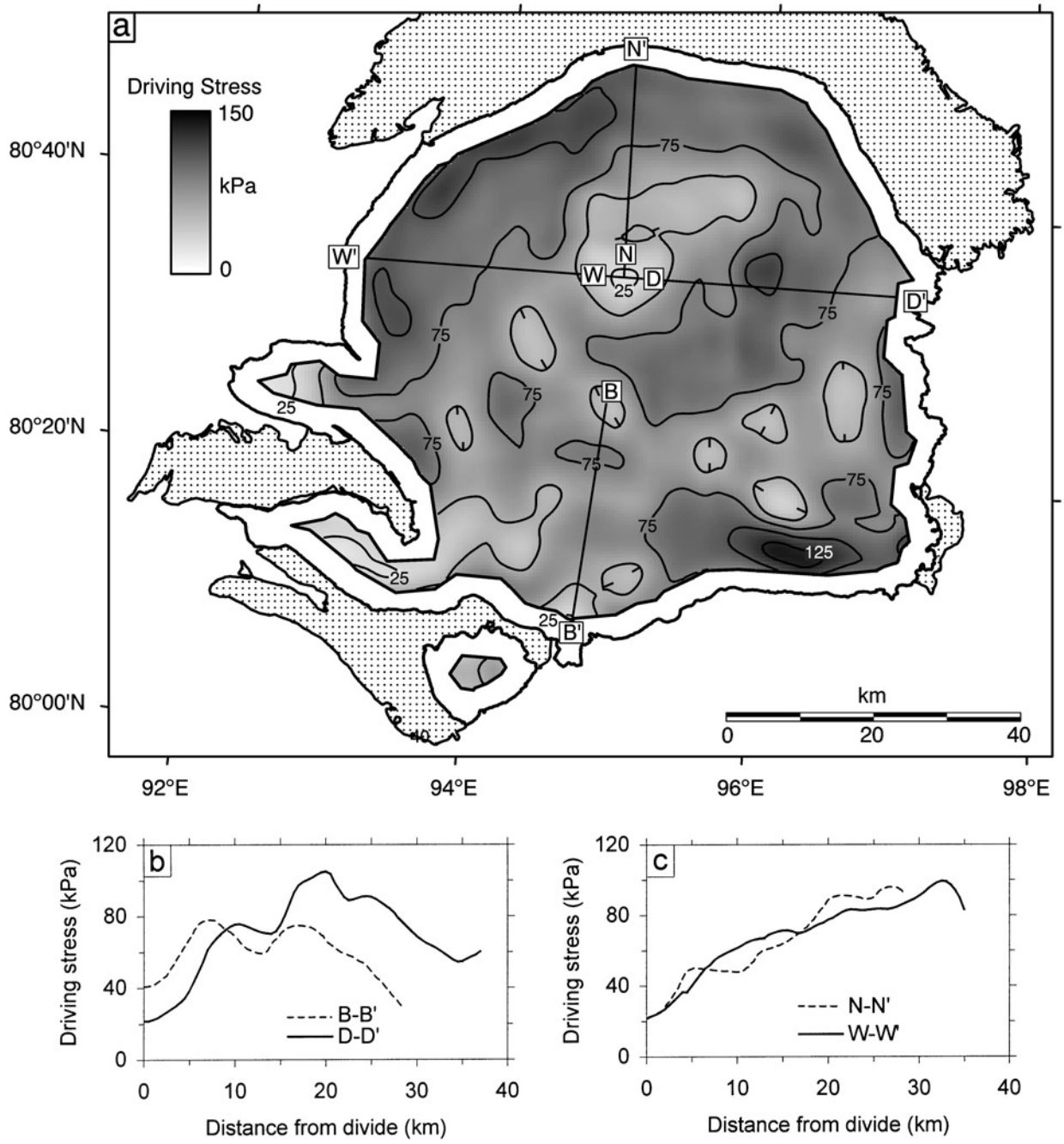

Figure 12. (a) Map of driving stresses (in kilopascals) on the Academy of Sciences Ice Cap, calculated using ice surface slope (α) averaged over a 5-km window (i.e., ~6 times the maximum ice thickness). (b) Driving stress profiles down ice streams 2 and 4 (B–B′ and D–D′, respectively) located in Figure 12a. (c) Driving stress profiles down two of low-velocity areas of the ice cap (N–N′ and W–W′ located in Figure 12a).

upper 54 m of a deep ice core taken at the ice cap crest have detected the 1963 maximum of artificial radioactivity from atmospheric nuclear tests, and ^{137}Cesium has defined the depth of the Chernobyl layer. The resulting mean annual net mass balance at this site, integrated over these periods, is 0.45 m yr^{-1} from 1963 and 0.55 m yr^{-1} from the 1986 horizon [*Fritzsche et al.*, 2001].

[40] Assuming a value of 0.3 m yr^{-1} as an average accumulation for the entire Academy of Sciences Ice Cap, because accumulation would be expected to decrease at lower elevations [*Bryazgin and Yunak*, 1988], this gives a total accumulation of 1.67 km^3 yr^{-1}. The volume of ice lost by iceberg calving from the ice cap is thus ~40% of total accumulation, implying that surface melting makes up ~60% or so. This assumes, of course, that the mass balance measurements on Vavilov Ice Cap, ~120 km to the south (Figure 1), which indicate that this ice cap is close to balance, can be extended northward.

[41] Variation of the mean accumulation over the Academy of Sciences Ice Cap by 0.05 m yr^{-1} around the estimate of 0.3 m yr^{-1} would alter the total mass input by ±0.28 km^3 yr^{-1}. This represents between 34 and 47% of the mass loss from the ice cap, assuming equilibrium. Even if the value of 0.45 m yr^{-1} recorded at the ice cap crest is used, this still yields a very conservative estimate of

26% of mass loss through iceberg production. These order-of-magnitude calculations of ice flux from the whole of the seaward margin of the Academy of Sciences Ice Cap provide, for the first time, an estimate of the likely contribution of iceberg production to the mass loss from a large Arctic ice cap.

5.4. Driving Stresses From Radar-Derived Data

[42] The pattern of driving stresses (τ) within the Academy of Sciences Ice Cap is calculated from the data on surface slope (α) and ice thickness (h) in the radar-derived digital elevation models (Figures 5 and 6). The driving stresses mapped in Figure 12 are calculated using the equation $\tau = \rho_i\, g\, h \sin \alpha$, where ρ_i is ice density and g is the acceleration due to gravity. The absolute values of calculated driving stress will vary with the amount of smoothing of the ice surface slopes [*Paterson*, 1994], but the spatial pattern of the stresses will remain unaltered. Driving stresses are generally lowest close to the ice divides on the ice cap (Figure 4) and also in one of the fast flow units, where they reach less than 40 kPa (Figure 12b). Although low in relative terms, these driving stresses are significantly higher than those recorded in the ice streams of West Antarctica [e.g., *Cooper et al.*, 1983; *Bentley*, 1987]. Maximum driving stresses, of between ~100 and 130 kPa, are found in several regions close to the ice margin (Figure 12), where the ice surface velocity is also low (Figure 10).

[43] The combination of relatively low driving stresses and high velocities in the ice streams on the ice cap indicates that ice motion in these areas is likely to be taking place not only by internal deformation, accounting for a few meters per year at most [*Paterson*, 1994], but also contains a significantly larger basal component. Given that ~50% of the ice cap bed lies below present sea level and ends in marine waters (Figures 7 and 8), it is likely that much of the bed is made up of deformable marine sediments and that basal motion may well involve this substrate.

[44] Finally, it should also be noted that driving stresses around the ice cap margin are not as low as those for the 1,100-km^2 drainage basin of Bråsvellbreen on the Austfonna ice cap in the neighboring archipelago of Svalbard (Figure 1). Bråsvellbreen surged in the 1930s [*Schytt*, 1969] and has a marginal driving stress of only 15–30 kPa combined with a very low ice surface velocity [*Dowdeswell*, 1986; *Dowdeswell et al.*, 1999]. This provides further evidence that the drainage basins on the Academy of Sciences Ice Cap are not of surge type.

6. Site Survey for Deep Ice Core Drilling

[45] There are few high-quality deep ice core records of paleoclimate from the Eurasian High Arctic [*Tarussov*, 1992; *Koerner*, 1997]. The Academy of Sciences Ice Cap in Severnaya Zemlya provides a particularly suitable site for deep drilling because (1) it is in the driest part of the glacierized Eurasian sector [*Dowdeswell*, 1995] thus yielding a particularly long record; (2) it is in the coldest area, and its physical and chemical stratigraphy is therefore likely to be affected less by melting-refreezing effects, including fractionation and percolation, than other Eurasian Arctic ice cores [e.g., *Dowdeswell et al.*, 1990; *Koerner*, 1997]; and (c) its ice thickness is among the deepest in the archipelago.

[46] Our airborne radar investigations provide detailed information on ice thickness (Figure 6), bed morphology (Figure 7), and ice flow conditions (Figure 10) that are of importance in the location of a drill site on Severnaya Zemlya. Guided by the work presented above, deep ice core drilling close to the crest of the Academy of Sciences Ice Cap at 80°31′N, 94°49′E has been completed recently [*Fritzsche et al.*, 1999, 2001]. The ice core is 723.9 m in length, with a basal temperature of −8°C. The lowermost 3.8 m of the core is composed of silty ice, indicating that basal melting and refreezing has probably taken place in the past. The chronological and mass balance information derived from this ice core will provide important data for future numerical modeling studies of the ice cap, which we have begun.

7. Conclusions

[47] The Academy of Sciences Ice Cap, at 5,575 km^2, is the largest in Severnaya Zemlya and, in general, within the Russian Arctic archipelagos (Figure 1) [*Dowdeswell et al.*, 2001]. About 200 km, or 42%, of the ice margin terminates in marine waters. Airborne radio echo sounding at 100 MHz measured the surface topography, ice thickness, and bed elevations of the ice cap. Digital terrain models of these data are then used, together with digital Landsat imagery, to define ice cap drainage basins and, with ice surface velocities derived from synthetic aperture radar interferometry, to investigate the flow dynamics of the ice cap. Our main findings are as follows:

1. The ice cap has a single well-defined dome, whose crest rises to an elevation of 749 m and is displaced northward of its geographical center (Figure 5). The north and northwestern parts of the ice cap are relatively uniform in surface slope. The central divide of the ice cap and several major drainage basins are mapped from satellite imagery (Figure 4). The southern and eastern ice cap margins are cut by several troughs in the ice surface, separated by ice ridges (Figures 5 and 8). These troughs have relatively well-defined margins and contain ice that appears rough at a kilometer scale on Landsat imagery (Figure 4).

2. The total volume of the Academy of Sciences Ice Cap is ~2,184 km^3 or ~5.5 mm of sea level equivalent. The thickest ice is located in two areas close to the ice cap center, and maximum ice thickness is 819 m (Figure 6). There is a clearly defined subglacial valley running east-west beneath the ice cap (Figure 7). About 50% of the bed is below sea level, with minimum bed elevations of over −200 m on the east side and more than −300 m in the southwest (Figure 7).

3. SAR interferometrically derived data on the velocity structure of the Academy of Sciences Ice Cap reveal the presence of several fast flowing units, or ice streams, that have a series of tightly spaced fringes at their lateral margins and extend back to within 5–10 km of the central crest of the ice cap (Figure 9). The central divide of the ice cap and the remainder of the margin have low velocities (Figure 10).

4. The ice streams are between 17 and 37 km in length and 4–8 km wide (Table 2). The mass flux through each of these fast flowing units is calculated using radar-derived ice thickness (Figure 6) and interferometrically derived velocity measurements (Figures 9–11). Mass loss from these ice streams is between 0.03 and 0.37 km^3 yr^{-1} (Table 2), much of it through iceberg calving (Figures 4b and 4c).

5. Total iceberg flux from the ice cap is ~0.65 km^3 yr^{-1} and probably represents ~40% of the overall mass loss, with the remainder coming from surface melting. This is the first time that iceberg calving has been calculated for the whole of the margin of an Arctic ice cap.

6. Fast flow within the ice streams is likely to be through basal motion as well as internal deformation, which alone would account for a only few meters per year of movement [*Paterson*, 1994]. Given that ~50% of the ice cap bed lies below present sea level (Figures 7 and 8) and terminates in the adjacent seas (Figure 1), it is likely that much of the bed is made up of deformable marine sediments and that basal motion probably involves this substrate.

7. There is no evidence of any deformation of either large-scale ice structures or medial moraines on the Academy of Sciences Ice Cap (Figure 4), and marginal driving stresses (Figure 12) are higher than those of ice cap drainage basins known to have surged in neighboring Svalbard [*Dowdeswell*, 1986]. This information implies that there has been no surge activity on the ice cap in the recent past, a situation that appears typical of ice masses throughout the Russian Arctic islands [*Dowdeswell and Williams*, 1997].

8. The fact that the ice cap bed was identified on ~97% of airborne radio echo sounding records was important both for site selection of a location for deep ice core drilling and in providing a basal boundary condition for numerical modeling of the Academy of Sciences Ice Cap and its response to recent climate change.

[48] **Acknowledgments.** The research program was funded by the following institutions: U.K. Natural Environment Research Council (grants GR3/9958 and GST/02/2195); EU Environment Programme (grants ENV4-CT97-0490 and 0426); Alfred-Wegener-Institut, Germany; and Russian Fund for Fundamental Studies. We thank C. Smirnov, V. Potapinko, and A. Mazhaev for logistical organization in Severnaya Zemlya.

References

Barkov, N. I., D. Y. Bol'shiyanov, O. A. Gvozdik, O. L. Klement'yev, V. M. Makeyev, I. G. Moskalenko, V. Y. Potapenko, and R. I. Yunak, New data on the structure and development of the Vavilov Ice Dome, Severnaya Zemlya, *Mater. Glyatsiologicheskikh Issled. Khronika*, *75*, 35–41, 1992.

Bentley, C. R., Antarctic ice streams: A review, *J. Geophys. Res.*, *92*, 8843–8858, 1987.

Bogorodskiy, V. V., and B. A. Fedorov, Radar probing of Severnaya Zemlya glaciers, in *The Physics of Ice*, edited by V. V. Bogorodskiy, pp. 1–16, Natl. Tech. Inf. Serv., Springfield, Va., 1971.

Bogorodskiy, V. V., C. R. Bentley, and P. E. Gudmandsen, *Radioglaciology*, 254 pp., D. Reidel, Norwell, Mass., 1985.

Bryazgin, N. N., and R. I. Yunak, Air temperature and precipitation on Severnaya Zemlya during ablation and accumulation periods, in *Geographical and Glaciological Studies in Polar Countries* (in Russian), edited by E. S. Korotkevich, and V. N. Petrov, pp. 70–81, Gidrometeoizdat, St. Petersburg, 1988.

Cattle, H., and J. Crossley, Modelling Arctic climate change, *Philos. Trans. R. Soc. London, Ser. A*, *352*, 201–213, 1995.

Cooper, A. P. R., Interface tracking in digitally recorded glaciological data, *Ann. Glaciol.*, *9*, 50–54, 1987.

Cooper, A. P. R., N. F. McIntyre, and G. D. Q. Robin, Driving stresses in the Antarctic Ice Sheet, *Ann. Glaciol.*, *3*, 59–64, 1983.

Dowdeswell, J. A., Drainage-basin characteristics of Nordaustlandet ice caps, Svalbard, *J. Glaciol.*, *32*, 31–38, 1986.

Dowdeswell, J. A., Glaciers in the High Arctic and recent environmental change, *Philos. Trans. R. Soc. London, Ser. A*, *352*, 321–334, 1995.

Dowdeswell, J. A., and R. L. Collin, Fast-flowing outlet glaciers on Svalbard ice caps, *Geology*, *18*, 778–781, 1990.

Dowdeswell, J. A., and N. F. McIntyre, The surface topography of large ice masses from Landsat imagery, *J. Glaciol.*, *33*, 16–23, 1987.

Dowdeswell, J. A., and M. Williams, Surge-type glaciers in the Russian High Arctic identified from digital satellite imagery, *J. Glaciol.*, *43*, 489–494, 1997.

Dowdeswell, J. A., D. J. Drewry, and J. C. Simoes, Comments on "6000-year climate records in an ice core from the Høghetta Ice Dome in northern Spitsbergen", *J. Glaciol.*, *36*, 353–356, 1990.

Dowdeswell, J. A., G. S. Hamilton, and J. O. Hagen, The duration of the active phase on surge-type glaciers: Contrasts between Svalbard and other regions, *J. Glaciol.*, *37*, 388–400, 1991.

Dowdeswell, J. A., M. R. Gorman, A. F. Glazovsky, and Y. Y. Macheret, Evidence for floating ice shelves in Franz Josef Land, Russian High Arctic, *Arct. Alp. Res.*, *26*, 86–92, 1994.

Dowdeswell, J. A., A. F. Glazovsky, and Y. Y. Macheret, Ice divides and drainage basins on the ice caps of Franz Josef Land, Russian High Arctic, defined from Landsat, Russian KFA-1000 and ERS-1 SAR satellite imagery, *Arct. Alp. Res.*, *27*, 264–270, 1995.

Dowdeswell, J. A., A.-M. Nuttall, B. Unwin, and D. J. Wingham, Velocity structure, flow instability and mass flux on a large Arctic ice cap from synthetic aperture radar interferometry, *Earth Planet. Sci. Lett.*, *167*, 131–140, 1999.

Dowdeswell, J. A., E. K. Dowdeswell, M. Williams, and A. F. Glazovsky, The glaciology of the Russian High Arctic from Landsat imagery, *U.S. Geol. Surv. Prof. Pap., 1386-F*, in press, 2002.

Fritzsche, D., L. M. Savatyugin, U. Ruth, F. Wilhelms, H. Miller, and H.-W. Hubberten, A new ice core drilled on Academy of Sciences Ice Cap, Severnaya Zemlya: First results (abstract), in *Terra Nostra*, p. 31, Alfred-Wegener-Stiftung, Berlin, Germany, 1999.

Fritzsche, D., F. Wilhelms, L. M. Savatyugin, J. F. Pinglot, H. Meyer, H.-W. Hubberten, and H. Miller, A new deep ice core from the Academy of Sciences Ice Cap, Severnaya Zemlya: First results, *Ann. Glaciol.*, in press, 2002.

Govorukha, L. S., Calculation of the average long-term budget of ice in the system of external mass exchange of the Severnaya Zemlya ice cover, *Articheskiy Antarkt. Nauchno-Issled. Inst. Trudy*, *294*, 12–27, 1970.

Govorukha, L. S., D. Y. Bol'shiyanov, V. S. Zarkhidze, L. Y. Pinchuk, and R. I. Yunak, Changes in the glacier cover of Severnaya Zemlya in the Twentieth Century, *Polar Geogr. Geol.*, *11*, 300–305, 1987.

Hambrey, M. J., and J. A. Dowdeswell, Flow regime of the Lambert Glacier-Amery Ice Shelf System, Antarctica: Structural evidence from Landsat imagery, *Ann. Glaciol.*, *20*, 401–406, 1994.

Hooke, R. L. B., *Principles of Glacier Mechanics*, 248 pp., Prentice-Hall, Englewoods Cliffs, N. J., 1998.

Isaaks, E. H, and R. M. Srivastava, *Applied Geostatistics*, 561 pp., Oxford Univ. Press, New York, 1989.

Joughin, I., S. Tulaczyk, M. Fahnstock, and R. Kwok, A mini-surge on the Ryder Glacier, Greenland, observed by satellite radar interferometry, *Science*, *274*, 228–230, 1996.

Koerner, R. M., Some comments on climatic reconstructions from ice cores drilled in areas of high melt, *J. Glaciol.*, *43*, 90–97, 1997.

Koryakin, V. S., Decrease in glacier cover on the islands of the Eurasian Arctic during the Twentieth Century, *Polar Geogr. Geol.*, *10*, 157–165, 1986.

Kotlyakov, V. M., Glaciers of the former Soviet Union, *U.S. Geol. Surv. Prof. Pap., 1386-F*, in press, 2002.

Kotlyakov, V. M., I. M. Korotkov, V. I. Nikolayev, V. N. Petrov, N. I. Barkov, and O. L. Klement'yev, Reconstruction of the Holocene climate from the results of ice-core studies on the Vavilov Dome, Severnaya Zemlya, *Mater. Glyatsiologicheskikh Issled.*, *67*, 103–108, 1989.

Kotlyakov, V. M., V. S. Zagorodnov, and V. I. Nikolayev, Drilling on ice caps in the Soviet Arctic and on Svalbard and prospects of ice core treatment, in *Arctic Research: Advances and Prospects*, vol. 2, edited by V. M. Kotlyakov, and V. Y. Sokolov, pp. 5–18, Nauka, Moscow, 1990.

Liestøl, O., Glaciers of Svalbard, Norway, *U.S. Geol. Surv. Prof. Pap.*, *1386-E*, 127–151, 1993.

Martin, P. J., and T. J. O. Sanderson, Morphology and dynamics of ice rises, *J. Glaciol.*, *25*, 33–45, 1980.

Massonnet, D., M. Rossi, C. Carmona, F. Adragna, G. Peltzer, K. Feigl, and T. Rabaute, The displacement field of the Landers earthquake mapped by radar interferometry, *Nature*, *364*, 138–142, 1993.

Meier, M. F., and A. S. Post, What are glacier surges?, *Can. J. Earth Sci.*, *6*, 807–817, 1969.

Paterson, W. S. B., *The Physics of Glaciers*, 3rd ed., Pergamon, Tarrytown, N. Y., 1994.

Schytt, V., Some comments on glacier surges in eastern Svalbard, *Can. J. Earth Sci.*, *6*, 867–873, 1969.

Smith, B. M. E., and S. Evans, Radio echo sounding: Absorption and scattering by water inclusions and ice lenses, *J. Glaciol.*, *11*, 133–146, 1972.

Tarussov, A., The Arctic from Svalbard to Severnaya Zemlya: Climatic reconstructions from ice cores, in *Climate Since A.D. 1500*, edited by R. S. Bradley and P. D. Jones, pp. 505–516, Routledge, New York, 1992.

Vaikmyae, R. A., and Y. M. K. Punning, Isotope and geochemical investigations on the Vavilov Glacier Dome, Severnaya Zemlya, *Polar Geogr. Geol.*, *8*, 73–79, 1982.

Zagorodnov, V. S., L. M. Savatyugin, and V. A. Morev, Temperature regime of the Academy of Sciences Ice Cap, Severnaya Zemlya, *Mater. Glyatsiologicheskikh Issled. Khronika Obsuzhdeniya*, *65*, 134–138, 1989.

Zebker, H. A., C. L. Werner, P. A. Rosen, and S. Hensley, Accuracy of topographic maps derived from ERS-1 interferometric radar, *IEEE Trans. Geosci. Remote Sens.*, *32*, 823–836, 1994.

Zinger, Y. M., and V. S. Koryakin, Est' li shel'fovyye ledniki na Severnoy Zemle? (Are there ice shelves on Severnaya Zemlya?), *Mater. Glyatsiologicheskikh Issled. Khronika Obsuzhdeniya*, *11*, 250–253, 1965.

R. P. Bassford, Centre for Polar Observation and Modeling, Bristol Glaciology Centre, School of Geographical Sciences, University of Bristol, Bristol BS8 1SS, UK.

J. A. Dowdeswell and M. R. Gorman, Scott Polar Research Institute, University of Cambridge, Lensfield Road, Cambridge CB2 1ER, UK. (jd16@cam.ac.uk)

A. F. Glazovsky and Y. Y. Macheret, Institute of Geography, Russian Academy of Sciences, Staromonetny 29, Moscow, Russia.

H.-W. Hubberten and H. Miller, Alfred-Wegener-Institut für Polar- und Meeresforschung, Columbusstrasse, D-27515 Bremerhaven, Germany.

L. M. Savatyuguin, Arctic and Antarctic Research Institute, St. Petersburg, Russia.

A. P. Shepherd, Centre for Polar Observation and Modelling, Department of Space and Climate Physics, University College London, 17–19 Gordon Street, London WC1E 6BT, UK.

Y. V. Vasilenko, Institute of Scientific Instruments, Uzbekistan Academy of Sciences, Tashkent, Uzbekistan.

M. Williams, Department of Geomatics, University of Newcastle, Newcastle-upon-Tyne NE1 7RU, UK.

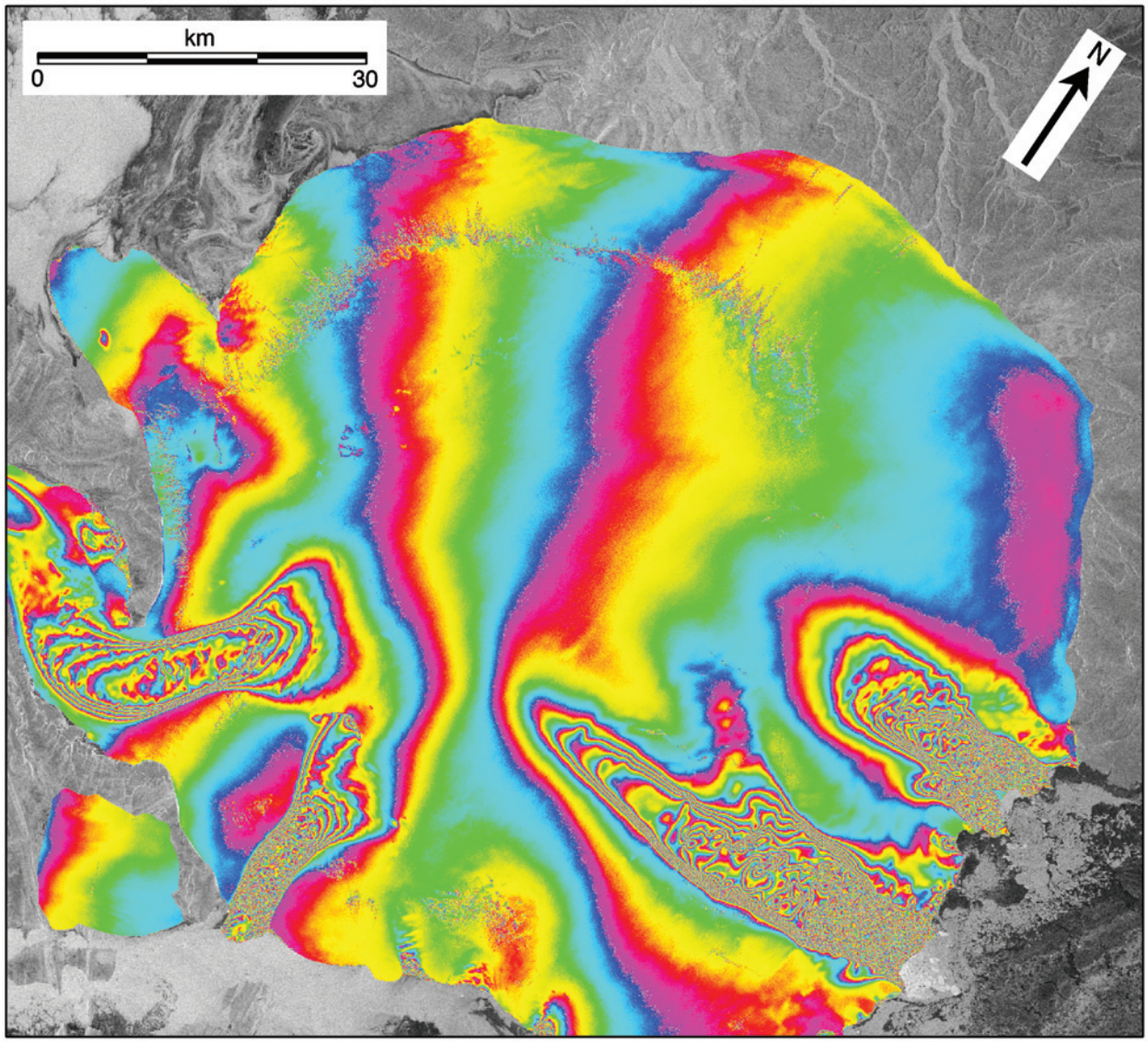

Figure 9. Synthetic aperture radar (SAR) interferorgram of the Academy of Sciences Ice Cap in the slant range geometry of the ERS satellite. The pair of SAR images were acquired on September 23 and 24, 1995, during the ERS tandem phase. The interferometric parallel baseline between the two satellite locations is 1 m. The ramp across the interferogram has been removed during subsequent processing. The interferogram of the ice cap is superimposed on a Landsat image of the surrounding terrain and marine waters.